Title

Localization of α1-2 fucose glycan in the mouse olfactory pathway

Authors

Daisuke Kondoh[a], Akihiro Kamikawa[b], Motoki Sasaki[a], Nobuo Kitamura[a]

Affiliation

[a]Laboratory of Veterinary Anatomy and [b]Laboratory of Veterinary Physiology, Department of Basic Veterinary Medicine, Obihiro University of Agriculture and Veterinary Medicine, Hokkaido, Japan

Running Head

Alpha1-2 fucose in mouse olfactory pathway

Corresponding Author

Daisuke Kondoh

Laboratory of Veterinary Anatomy, Department of Basic Veterinary Medicine

Obihiro University of Agriculture and Veterinary Medicine

Inada-cho, Obihiro, Hokkaido 080-8555 (Japan)

Tel: 0155-49-5369 Email: kondoh-d@obihiro.ac.jp

Key words: alpha1-2 fucose; accessory olfactory bulb; anterior olfactory nucleus; glycosylation; lateral olfactory tract; main olfactory bulb; olfactory epithelium; olfactory tubercle; piriform cortex; *Ulex europaeus* agglutinin-I; vomeronasal epithelium

Abstract

Glycoconjugates in the olfactory system play critical roles in neuronal formation, and α1–2 fucose (α1–2Fuc) glycan mediates neurite outgrowth and synaptic plasticity. Histochemical findings of α1–2Fuc glycan in the mouse olfactory system detected using *Ulex europaeus* agglutinin-I (UEA-I) vary. The present study histochemically assessed the main olfactory and vomeronasal pathways in male and female ICR and C57BL/6J mice aged 3- to 4-months using UEA-I. *Ulex europaeus* agglutinin-I reacted with most receptor cells arranged mainly at the basal region of the olfactory epithelium. The olfactory nerve layer and glomerular layer of the main olfactory bulb were speckled with positive UEA-I staining, and positive fibers were scattered from the glomerular to the internal plexiform layer. The lateral olfactory tract and rostral migratory stream were also positive for UEA-I. We identified at least superficial short-axon cells, interneurons of the external plexiform layer, external, middle and internal tufted cells, mitral cells and granule cells as the origins of the UEA-I-positive fibers in the main olfactory bulb. The anterior olfactory nucleus, anterior piriform cortex and olfactory tubercle were negative for UEA-I. Most receptor cells in the vomeronasal epithelium and most glomeruli of the accessory olfactory bulb were positive for UEA-I. The present findings indicated that α1–2Fuc glycan is located within the primary and secondary, but not the ternary, pathways of the main olfactory system, in local circuits of the main olfactory bulb and within the primary, but not secondary, pathway of the vomeronasal system.

List of abbreviation	
α1–2Fuc	α1–2 fucose
AOB	accessory olfactory bulb
LOT	lateral olfactory tract
MOB	main olfactory bulb
NCAM	neural cell adhesion molecule
OE	olfactory epithelium
RMS	rostral migratory stream
UEA-I	*Ulex europaeus* agglutinin-I
VNE	vomeronasal epithelium

Introduction

Odoriferous compounds are recognized mainly by receptor cells in the olfactory epithelium (OE) of most mammals. These receptor cells project axons as the olfactory nerve to the glomeruli in the main olfactory bulb (MOB) and form synaptic contacts with the dendrites of secondary olfactory neurons, namely mitral and tufted cells. These secondary neurons project axons to the olfactory cortex region in rodents, including the anterior olfactory nucleus, anterior and posterior piriform cortex and olfactory tubercle, through the lateral olfactory tract (LOT) [Giessel and Datta, 2014]. On the other hand, the vomeronasal system of most mammals is stimulated mainly by species-specific substances, and this pathway is separated from the main olfactory pathway. Receptor cells of the vomeronasal epithelium (VNE) in the vomeronasal organ project axons as the vomeronasal nerve to the glomeruli in the accessory olfactory bulb (AOB) and form synapses with secondary vomeronasal neurons [Brignall and Cloutier, 2015].

At the histological level, the OE generally comprised supporting, receptor and basal progenitor cell types with nuclei located in the apical, middle and basal regions of the OE, respectively. The VNE of mice comprised supporting cells with nuclei located in the apical region, receptor cells expressing vomeronasal receptor 1 and 2 located in the middle and basal regions, respectively, and progenitor cells located in the marginal region with non-sensory epithelium [Halpern and Martínez-Marcos, 2003]. The MOB was generally divided into 6 layers; olfactory nerve, glomerular, external plexiform, mitral cell, internal plexiform and granule cell layers, while the AOB comprised 5 layers; vomeronasal nerve, glomerular, external plexiform, internal plexiform and granule cell layers.

Glycosylation affects the functional properties of proteins and lipids in various

tissues, including the central nervous system. Sugar chains in the MOB play critical roles in neuronal formation [Plendl and Sinowatz, 1998], and the abundance of glycoconjugate moieties varies among developmental stages in the MOB [Tisay et al., 2002] and in the AOB [Salazar and Sánchez Quinteiro, 2003]. Neuronal functions, such as learning and memory, as well as neuronal morphological changes, including neurite outgrowth and synaptic plasticity are mediated by α1–2 fucose (α1–2Fuc) glycan [Pohle et al., 1987; Krug et al., 1991, 1994; Matthies et al., 1996; Lorenzini et al., 1997; Kalovidouris et al., 2005; Murrey et al., 2006]. Murrey et al. [2009] found that development of the olfactory bulb is defective in mice with a deficiency of α1–2-specific fucosyltransferase 1, and we recently showed that the amount of α1–2Fuc glycan in the olfactory bulb diurnally fluctuates via rhythmic expression of the *Fut1* gene [Kondoh et al., 2014]. Therefore, α1–2Fuc glycan might control functional changes in the olfactory system during developmental stages and circadian variations.

Although α1–2Fuc glycan has been histochemically localized in the mouse olfactory system using *Ulex europaeus* agglutinin-I (UEA-I) [Lundh et al., 1989; Ducray et al., 1999; Salazar et al., 2001; Lipscomb et al., 2002, 2003; Salazar and Sánchez Quinteiro, 2003; Murrey et al., 2009; Barrios et al., 2014; Kondoh et al., 2014], the findings are diverse. For example, we showed that α1–2Fuc glycan preferentially locates in the LOT and in the glomerular layer of the AOB of the ICR mouse [Kondoh et al., 2014], whereas others have not found that UEA-I reacts with the mouse LOT. Because of the potential of α1–2Fuc glycan as described above, identifying the histological components and cell types that α1–2Fuc glycan modifies in the olfactory system is important. We therefore histochemically analyzed the olfactory pathway of ICR and C57BL/6J mice using UEA-I.

Materials and Methods

Animals

Nineteen mice (age, 3- to 4-months; Japan SLC) were maintained under a 12-h light: 12-h dark cycle (lights on at 08:00) at a controlled ambient temperature of 22 ± 1°C and sacrificed between 18:00 and 20:00 as described below. This study proceeded according to the Regulations on Management and Operation of Animal Experiments, and the Animal Care and Use Committee of Obihiro University of Agriculture and Veterinary Medicine approved the experimental protocol (approval numbers, 26-89 and 27-20).

Preparation of sections

Six male and two female ICR and three male and two female C57BL/6J mice were anesthetized via an intraperitoneal injection of pentobarbital (0.20 mg/g body weight) and sacrificed by cardiac perfusion with Bouin's fixative. The OE, olfactory bulb and brain including the olfactory cortex were embedded in paraffin and cut into 5-μm thick sections. The olfactory bulbs of three male ICR and the remaining ten mice were sectioned frontally and sagittally, respectively, deparaffinized, rehydrated and then processed for UEA-I histochemistry. Six other male ICR mice were anesthetized via an intraperitoneal injection of pentobarbital and sacrificed by cardiac perfusion with 4% paraformaldehyde. The vomeronasal organs of three mice were embedded in paraffin and cut frontally into 5-μm thick sections, and then the olfactory bulbs were embedded in OCT compound (Sakura Finetek, Tokyo, Japan) and cut sagittally into 15-μm thick sections in a cryostat. The olfactory bulbs of three other mice were sliced sagittally into 50-μm thick sections using a microslicer (Dosaka, Tokyo, Japan).

UEA-I histochemistry

Sections were incubated with 0.3% H_2O_2 in methanol to eliminate endogenous peroxidase. The sections were rinsed in phosphate buffered saline (0.01 M, pH 7.4) and then nonspecific reactions were blocked by incubating the sections with 1% bovine serum albumin. The sections were incubated with 20 μg/mL of biotinylated UEA-I L8262 (Sigma-Aldrich, St. Louis, MO, USA) or B-1065 (Vector Laboratories, Burlingame, CA, USA) at 4°C overnight and reacted with the avidin-biotin-peroxidase complex reagent PK-6100 (Vector) for 30 min. Thereafter, the sections were colored with Tris-HCl buffer (0.05 M, pH 7.4) containing 0.006% H_2O_2 and 0.02% 3-3'-diaminobenzidine tetrahydrochloride. Control sections were stained after UEA-I was absorbed with 0.5 M L-fucose.

Anti-olfactory marker protein (OMP) immunohistochemistry

Sections adjacent to those used in UEA-I histochemistry were incubated with 0.3% H_2O_2 in methanol to eliminate endogenous peroxidase. The sections were rinsed in phosphate buffered saline and incubated with 3% normal goat serum to block nonspecific reactions. The sections were incubated at 4°C overnight with 2 μg/mL of sc-67219 primary anti-OMP antibody raised in rabbits (Santa Cruz Biotechnologies, Santa Cruz, CA, USA), followed by 7.5 μg/mL of BA-1000 biotinylated anti-rabbit IgG antibody raised in goats (Vector) for 60 min, and then with avidin-biotin-peroxidase complex for 30 min. Thereafter, sections were colored with Tris-HCl buffer containing 0.006% H_2O_2 and 0.02% 3-3'-diaminobenzidine tetrahydrochloride.

Results

Sex and strain differences among histological components and cell types that bound to UEA-I were not evident between ICR and C57BL/6J mice. The methods used to prepare the sections did not affect either the MOB or the AOB (online suppl. fig. 1).

UEA-I reaction in the OE

The OE covered the dorsocaudal part of the nasal cavity, and the thickness differed according to location; the dorsal OE was thicker than the ventral OE (fig. 1). In both the dorsal and ventral OE, UEA-I reacted with most receptor cells arranged mainly at the basal area of the middle region, and dendrites and axon bundles of these receptor cells were also positive for UEA-I (fig. 1a, b). Anti-OMP antibody reacted intensely with UEA-I-negative receptor cells but faintly with UEA-I-positive receptor cells (fig. 1c, d). Several cells scattered in the supporting cell layer also stained positive for UEA-I (fig. 1a, b, double arrowheads), but most supporting and basal cells (fig. 1a, b, arrowheads) were not stained.

UEA-I reaction in the MOB

Dappled UEA-I reactions with the olfactory nerve and glomerular layers were identified in sagittal sections (fig. 2a, b, 3a), and the degree of the reaction varied from none to intense among the glomeruli (fig. 2b, c). Some UEA-I-positive fibers were scattered from the glomerular to the mitral cell layer, and many positive fibers were identified in the internal plexiform layer (fig. 2b). Thick fiber bundles, namely the LOT and the rostral migratory stream (RMS), were positive in the granule cell layer (fig. 2b). These positive reactions were suppressed after absorbing UEA-I with L-fucose (fig. 2d,

e). Frontal sections of the rostral area (fig. 3b, c) lacked appararent UEA-I-positive fibers from the glomerular to the granule cell layer, although the olfactory nerve layer and in several glomeruli reacted with UEA-I. The UEA-I-positive LOT and RMS were distinctly located at frontal sections of the caudal area (fig. 3d)

At least seven cell types were identified according to a classification summarized by Nagayama et al. [2014] as the origins of the UEA-I-positive fibers in the MOB. Fibers that were UEA-I-positive in the glomerular layer were derived from superficial short-axon cells (soma size, ~ 10 μm; fig. 4a) and external tufted cells (~ 12 μm; fig. 4b), and some of these fibers encircled, but did not penetrate individual glomeruli. In the external plexiform layer, axons and dendrites of both the middle (~ 20 μm; fig. 4c) and internal tufted cells (~ 20 μm; fig. 4e, h) and fibers derived from interneurons (~ 10 μm; fig. 4d) were reactive. Mitral cells (~ 20 μm; fig. 4f, h) in the mitral cell layer also contained the UEA-I-positive dendrites and axons that joined positive fiber bundles in the internal plexiform and granule cell layers, and fibers derived from granule cells between the mitral and granule cell layers (~ 7 μm; fig. 4g) were also reactive.

UEA-I reaction in the olfactory cortex

We found that UEA-I did not react with the anterior olfactory nucleus, anterior piriform cortex and olfactory tubercle (fig. 5). The LOT and RMS within the same sections was positive for UEA-I.

UEA-I reaction in the vomeronasal organ

The vomeronasal organ possessed the VNE, non-sensory epithelium and connective tissue containing vessels, glands and peripheral vomeronasal nerves, and

UEA-I reacted with the VNE, vomeronasal nerves and mucous layer covering the VNE and non-sensory epithelium (fig. 6a). The cell membranes of most receptor cells located in both the middle (fig. 6b, arrows) and basal (fig. 6b, arrowheads) regions were positive for UEA-I, although the large cell bodies of these cells located in the basal region were negative (fig. 6b). Although the receptor cells clustered near the marginal region were intensely positive for UEA-I, cells that are situated in the region of progenitor cells, i.e. the marginal zone, were negative (fig. 6c).

UEA-I reaction in the AOB

Sagittal sections from all sixteen mice showed that UEA-I significantly reacted with the vomeronasal nerve layer, the glomerular layer and the LOT, which is located within the internal plexiform layer of the AOB, but not the other layers (fig. 7). Among the 16 ICR mice, the UEA-I reaction was region-specific in only one female after cutting with a microslicer and two males after paraffin embedding; the rostral glomeruli were intensely positive and the anterior and posterior caudal glomeruli were weakly and moderately positive, respectively (fig. 7b), whereas the glomeruli of the other ICR or C57BL/6 mice reacted intensely and uniformly with UEA-I (fig. 7a).

Discussion

Alpha1–2Fuc glycan mediates neuronal functions, affects neuronal morphology [Pohle et al., 1987; Krug et al., 1991, 1994; Matthies et al., 1996; Lorenzini et al., 1997; Kalovidouris et al., 2005; Murrey et al., 2006] and also might control olfactory functions according to developmental stage [Murray et al., 2009] and circadian rhythms [Kondoh et al., 2014]. We showed that most receptor cells arranged at the basal region of the OE possess dendrites and axons including α1–2Fuc glycan, which agrees with the findings reported by Ducray et al. [1999]. The basal cells in the OE differentiate into receptor cells and mature while moving from the basal to the apical region. We also showed that UEA-I-positive receptor cells possess scant OMP, a marker of mature olfactory receptor cells, suggesting that the positive cells at the basal region are immature receptor cells that extend axons to the MOB. Glycoconjugates including α1–2Fuc glycan were also located at the olfactory nerve layer and in several glomeruli of the MOB that are targets for axon endings of olfactory receptor cells, as reported by Lipscomb et al. [2002, 2003], Salazar and Sánchez Quinteiro [2003] and Murrey et al. [2009]. These findings suggest that α1–2Fuc glycan is associated with dendrite and neurite outgrowths within the primary pathway of the main olfactory system.

The present study found several UEA-I-positive cells scattered throughout the supporting cell layer of the OE. Although these cells might correspond to some types of microvillar olfactory cells that comprise at least five cell types, their functions remain unknown [Elsaesser and Paysan, 2007], and further studies are needed to elucidate which types of microvillar olfactory cells possess glycoconjugates including α1–2Fuc glycan.

Some neuronal fibers including α1–2Fuc glycan were scattered from the glomerular to the internal plexiform layer in the MOB, and at least seven cell types were

identified as the origins of these fibers. Among them, superficial short-axon cells, some external tufted cells, interneurons in the external plexiform layer and granule cells mediate local neuronal circuits [Nagayama et al., 2014]. On the other hand, the middle tufted cells, internal tufted cells and mitral cells function as projective neurons of the MOB, and extend axons to the olfactory cortex through the LOT [Giessel and Datta, 2014]. The present study also located a large amount of α1–2Fuc glycan at the LOT. Therefore, glycoconjugates including α1–2Fuc glycan are located in both local circuits of the MOB and the secondary pathway of the olfactory system. Neural cell adhesion molecule (NCAM) is a highly glycosylated protein [Liedtke et al., 2001] and apparently the main core protein of α1–2Fuc glycan in the mouse olfactory bulb [Pestean et al., 1995; Murrey et al., 2009; Kondoh et al., 2014], and it plays critical roles in neurite outgrowth and synaptic formation, especially in the olfactory bulb [Treloar et al., 1997; Zamze et al., 1998; Perlson et al., 2013]. Because α1–2Fuc glycan also mediates neuronal functions and affects neuronal morphology [Pohle et al., 1987; Krug et al., 1991, 1994; Matthies et al., 1996; Lorenzini et al., 1997; Kalovidouris et al., 2005; Murrey et al., 2006], α1–2Fuc attachments might affect NCAM function and mediate both major adjustments within the olfactory pathway and minor adjustments within the MOB.

The histological localization of α1–2 fucose at various sites within the olfactory system using UEA-I [Lundh et al., 1989; Ducray et al., 1999; Lipscomb et al., 2002, 2003; Salazar et al., 2001; Salazar and Sánchez Quinteiro, 2003; Murrey et al., 2009; Barrios et al., 2014; Kondoh et al., 2014] might depend on differences in sex, age, mouse strain, method preparing sections, UEA-I batch, fixative, the method used to detect positive reactions and/or cutting angles. Furthermore the time of the day when the mice are sacrificed might affect not only the amount of α1–2Fuc glycan but also its localization in

the MOB, although our preliminary prolonged staining with UEA-I-staining showed that UEA-I-binding regions are similar at the layer level during the daytime and nighttime (data not shown). The present findings did not differ between the sexes, mouse strains (ICR vs. C57BL/6J), UEA-I products (L8262 vs. B-1065) and preparing sections by paraffin embedding, freezing or cutting with a microslicer. Our preliminary findings also indicated that UEA-I binding is not affected by any of 4% paraformaldehyde, or Bouin's or Zamboni's fixatives (data not shown) or by detection using avidin-biotin-peroxidase complex or fluorescence labelling (data not shown). Although the results did not differ between ICR and C57BL/6J mice in the present study, Salazar et al. [2001] found that UEA-I does not react with the MOB of adult BALB/c mice, suggesting that strain differences are involved. Because Barrios et al. [2014] also described that UEA-I does not react with the OE or with the MOB of BALB/c mice > 10 months, age might also affect UEA-I histochemistry in the olfactory system. In fact, Tisay et al. [2002] described that another glycan structure detected by the lectin, *Dolichos biflorus* agglutinin is included in the secondary olfactory pathway of BALB/c, but not C57BL/6, CBA or Quackenbush mice. Comparative studies between age groups and mouse strains other than ICR and C57B/6J are required to address this issue.

We showed that α1–2Fuc glycan is included in some neuronal fibers from the glomerular to the granule cell layer in the MOB. However, only one study has identified UEA-I-positive fibers in the LOT [Kondoh et al., 2014]. To establish the cause of this difference from other reports, we evaluated UEA-I staining in sections of the frontal MOB. We did not easily found UEA-I-positive fibers from the glomerular to the granule cell layer in frontal sections of the rostral area, suggesting that cutting these fibers vertically or in parallel can affect the profiles of structures in the MOB.

We showed that α1–2Fuc glycan is located on the cell membranes of not only immature receptor cells clustered near the marginal region but also most mature cells of the VNE in addition to most glomeruli of the AOB, which agrees with findings reported by Lundh et al. [1989]. These findings differ from observations of the main olfactory system indicating that a few mature receptor cells of the OE and several glomeruli of the MOB possess α1–2Fuc glycan. Because NCAM, which seems to be the main core protein of α1–2Fuc glycan in the olfactory system [Pestean et al., 1995; Murrey et al., 2009; Kondoh et al., 2014], is expressed in most receptor cells and glomeruli of both the main olfactory and vomeronasal systems [Yoshihara et al., 1997], the degree of α1–2-fucosylation of NCAM within mature receptor cells might differ between these pathways. This glycan might be associated with neuronal function in addition to neuronal outgrowths within the primary pathway of the vomeronasal system. On the other hand, both the secondary neurons and interneurons of the AOB were negative for UEA-I, suggesting that α1–2Fuc attachments do not mediate the secondary pathway of the vomeronasal system and the local circuit of the AOB.

Some studies [Lipscomb et al., 2003; Salazar and Sánchez Quinteiro, 2003; Barrios et al., 2014] have found that UEA-I reacts more intensely with rostral than caudal glomeruli in the AOB. Salazar and Sánchez Quinteiro [2003] as well as Barrios et al. [2014] have also reported that UEA-I reacts with receptor cells of the VNE that express vomeronasal receptor 1 in the middle region, but not with those express vomeronasal receptor 2 in the basal region. Because the rostral and caudal glomeruli of the mouse respectively receive input fibers from vomeronasal receptor cells expressing vomeronasal receptors 1 and 2, UEA-I has generally been regarded as an indicator of glomeruli that possess different properties. However, the present study found region-specific UEA-I

staining in the AOB of only three (two male and one female ICR) mice, compared with a uniform UEA-I reaction among the remaining thirteen mice. In addition, higher magnification of the UEA-I reaction in the VNE (fig. 6b) indicated that most receptor cells located in both the basal and middle regions possess UEA-I-positive cell membranes, whereas the findings at lower magnification (fig.6a) are similar to those of Salazar and Sánchez Quinteiro [2003] and Barrios et al. [2014]. We consider that the region-specific localization of α1–2Fuc glycan in the AOB differs among individuals and that this might be caused by the presence or absence of cues that activate receptor cells.

The present study localized glycoconjugates including α1–2Fuc glycan at the primary and secondary pathways of the main olfactory system, in local circuits of the MOB and at the primary pathway of the vomeronasal system, but not at the secondary pathway or in local circuits of the AOB. These findings suggest that α1–2Fuc glycan might mediate both major and minor adjustments in the main olfactory system, and that it might functionally differ between the main olfactory and vomeronasal pathways.

Acknowledgements

We thank the staff of the Laboratory Animal Center, Obihiro University of Agriculture and Veterinary Medicine for maintaining the animals. This study was partly supported by a Grant-in-Aid for Young Scientists (B) KAKENHI (15K20841) to DK from the Ministry of Education, Culture, Sports, Science and Technology (MEXT) of Japan. The authors declared no potential conflicts of interest with respect to the research, authorship and/or publication of this article.

References

Barrios, A.W., G. Núñez, P. Sánchez Quinteiro, I. Salazar (2014) Anatomy, histochemistry, and immunohistochemistry of the olfactory subsystems in mice. Front Neuroanat *8:* 63.

Brignall, A.C., J.F. Cloutier (2015) Neural map formation and sensory coding in the vomeronasal system. Cell Mol Life Sci *72:* 4697–4709.

Ducray, A., A. Propper, A. Kastner (1999) Detection of alpha-L fucose containing carbohydrates in mouse immature olfactory neurons. Neurosci Lett *274:* 17–20.

Elsaesser R., J. Paysan (2007) The sense of smell, its signalling pathways, and the dichotomy of cilia and microvilli in olfactory sensory cells. BMC Neurosci *8:* S1.

Giessel A.J., S.R. Datta (2014) Olfactory maps, circuits and computations. Curr Opin Neurobiol *24:* 120−132.

Halpern, M., A. Martínez-Marcos (2003) Structure and function of the vomeronasal system: an update. Prog Neurobiol *70:* 245−318.

Kalovidouris, S.A., C.I. Gama, L.W. Lee, L.C. Hsieh-Wilson (2005) A role for fucose α(1–2) galactose carbohydrates in neuronal growth. J Am Chem Soc *127:* 1340–1341.

Kondoh, D., H. Tateno, J. Hirabayashi, Y. Yasumoto, R. Nakao, K. Oishi (2014) Molecular clock regulates daily α1–2-fucosylation of the neural cell adhesion molecule (NCAM) within mouse secondary olfactory neurons. J Biol Chem *289:* 36158–36165.

Krug, M., R. Jork, K. Reymann, M. Wagner, H. Matthies (1991) The amnesic substance 2-deoxy-D-galactose suppresses the maintenance of hippocampal LTP. Brain Res *540:* 237–242.

Krug, M., M. Wagner, S. Staak, K.H. Smalla (1994) Fucose and fucose-containing sugar epitopes enhance hippocampal long-term potentiation in the freely moving rat. Brain Res *643:* 130–135.

Liedtke, S., H. Geyer, M. Wuhrer, R. Geyer, G. Frank, R. Gerardy-Schahn, U. Zähringer, M. Schachner (2001) Characterization of N-glycans from mouse brain neural cell adhesion molecule. Glycobiology *11:* 373–384.

Lipscomb, B.W., H.B. Treloar, C.A. Greer (2002) Novel microglomerular structures in the olfactory bulb of mice. J Neurosci *22:* 766–774.

Lipscomb, B.W., H.B. Treloar, J. Klenoff, C.A. Greer (2003) Cell surface carbohydrates and glomerular targeting of olfactory sensory neuron axons in the mouse. J Comp Neurol *467:* 22–31.

Lorenzini, C.G., E. Baldi, C. Bucherelli, B. Sacchetti, G. Tassoni (1997) 2-Deoxy-D-galactose effects on passive avoidance memorization in the rat. Neurobiol Learn Mem *68:* 317–324.

Lundh, B., U. Brockstedt, K. Kristensson (1989) Lectin-binding pattern of neuroepithelial and respiratory epithelial cells in the mouse nasal cavity. Histochem J *21:* 33–43.

Matthies, H., S. Staak, M, Krug (1996) Fucose and fucosyllactose enhance *in vitro* hippocampal long-term potentiation. Brain Res *725:* 276–280.

Murrey, H.E., C.I. Gama, S.A. Kalovidouris, W.I. Luo, E.M. Driggers, B. Porton, L.C. Hsieh-Wilson (2006) Protein fucosylation regulates synapsin Ia/Ib expression and neuronal morphology in primary hippocampal neurons. Proc Natl Acad Sci USA *103:* 21–26.

Murrey, H.E., S.B. Ficarro, C. Krishnamurthy, S.E. Domino, E.C. Peters, L.C. Hsieh-Wilson (2009) Identification of the plasticity-relevant fucose-α(1–2)-galactose

proteome from the mouse olfactory bulb. Biochemistry *48:* 7261–7270.

Nagayama, S., R. Homma, F. Imamura (2014) Neuronal organization of olfactory bulb circuits. Front Neural Circuits *8:* 98.

Perlson, E., A.G. Hendricks, J.E. Lazarus, K. Ben-Yaakov, T. Gradus, M. Tokito, E.L. Holzbaur (2013) Dynein interacts with the neural cell adhesion molecule (NCAM180) to tether dynamic microtubules and maintain synaptic density in cortical neurons. J Biol Chem *288:* 27812–27824.

Pestean, A., I. Krizbai, H. Böttcher, A. Párducz, F. Joó, J.R. Wolff (1995) Identification of the *Ulex europaeus* agglutinin-I-binding protein as a unique glycoform of the neural cell adhesion molecule in the olfactory sensory axons of adults rats. Neurosci Lett *195:* 117–120.

Plendl, J., F. Sinowatz (1998) Glycobiology of the olfactory system. Acta Anat *161:* 234–253.

Pohle, W., L. Acosta, H. Rüthrich, M. Krug, H. Matthies (1987) Incorporation of [^{3}H]fucose in rat hippocampal structures after conditioning by perforant path stimulation and after LTP-producing tetanization. Brain Res *410:* 245–256.

Salazar, I., P. Sánchez Quinteiro, M. Lombardero, J.M. Cifuentes (2001) Histochemical identification of carbohydrate moieties in the accessory olfactory bulb of the mouse using a panel of lectins. Chem Senses *26:* 645–652.

Salazar, I., P. Sánchez Quinteiro (2003) Differential development of binding sites for four lectins in the vomeronasal system of juvenile mouse: from the sensory transduction site to the first relay stage. Brain Res *979:* 15–26.

Tisay, K.T., J.A. St. John, B. Key (2002) Expression of specific glycoconjugates in both primary and secondary olfactory pathways in BALB/C mice. J Comp Neurol *443:*

213–225.

Treloar, H., H. Tomasiewicz, T. Magnuson, B. Key (1997) The central pathway of primary olfactory axons is abnormal in mice lacking the N-CAM-180 isoform. J Neurobiol *32:* 643–658.

Yoshihara, Y., M. Kawasaki, A. Tamada, H. Fujita, H. Hayashi, H. Kagamiyama, K. Mori (1997) OCAM: A new member of the neural cell adhesion molecule family related to zone-to-zone projection of olfactory and vomeronasal axons. J Neurosci *17:* 5830–5842.

Zamze, S., D.J. Harvey, Y.J. Chen, G.R. Guile, R.A. Dwek, D.R. Wing (1998) Sialylated N-glycans in adult rat brain tissue: a widespread distribution of disialylated antennae in complex and hybrid structures. Eur J Biochem *258:* 243–270.

Figure Legends

fig. 1. UEA-I binding in olfactory epithelium. Sections from male ICR mouse processed using Bouin's fixative and paraffin embedding. Arrows with each digit indicate same nuclei within adjacent sections. **a** and **b** UEA-I staining in dorsal (**a**) and ventral (**b**) regions of nasal cavity. Arrowheads and double arrowheads, UEA-I-negative basal cells and UEA-I-positive cells scattered in supporting cell layer, respectively. Dashed line (**a**) indicates border between apical and basal regions with few and many positive cells, respectively. *Axon bundles of receptor cells. D, excretory duct; G, olfactory gland acinus; V, blood vessel. **c** and **d** Olfactory marker protein (OMP)-positive reactions (**c** and **d**) on sections adjacent to those shown in (**a** and **b**), respectively. Dashed line (**c**) indicates border between apical and basal regions with many and few intensely-positive cells, respectively. Bars = 20 μm.

fig. 2. UEA-I binding in sagittal section of olfactory bulb. Sections from male C57BL/6J mouse processed using Bouin's fixative and paraffin embedding. **a** Image of whole olfactory bulb. Left and upper, rostral and dorsal, respectively. Box shows magnified region in (**b**). AOB, accessory olfactory bulb; MOB, main olfactory bulb. **b** Higher magnification of MOB layer structure. EPL, external plexiform layer; GCL, granule cell layer; GL, glomerular layer; IPL, internal plexiform layer; MCL, mitral cell layer; ONL, olfactory nerve layer. Arrows and arrowhead, lateral olfactory tract and rostral migratory stream, respectively. **c** Higher magnification of intensely-positive (arrow) and negative (asterisks) glomeruli of MOB. **d and e** Preabsorption of UEA-I with L-fucose to suppress UEA-I binding to olfactory bulb (**d** and **e**) corresponds to (**a** and **b**), respectively. Bars = 500 (**a** and **d**) and 100 (**b**, **c** and **e**) μm.

fig. 3. UEA-I binding in frontal sections of olfactory bulb and olfactory cortex. Sections from male ICR mouse processed using Bouin's fixative and paraffin embedding. **a** Sagittal image of whole olfactory bulb. Dashed lines (b–d) correspond to sliced regions. Left and upper, rostral and dorsal, respectively. **b–d** Rostral (**b**), medial (**c**) and caudal (**d**) parts of olfactory bulb. Arrows and arrowheads, lateral olfactory tract and intensely-positive glomeruli, respectively. *Vomeronasal nerve layer and glomerular layer in accessory olfactory bulb. RMS, rostral migratory stream. Left and upper, medial and dorsal, respectively. Bars = 500 (**a**) and 300 (**b**–**d**) μm.

fig. 4. Cells of origins (arrows) and UEA-I-positive fibers (arrowheads) in main olfactory bulb. Sections from male C57BL/6J mouse processed using Bouin's fixative and paraffin embedding. **a** Superficial short-axon cells in glomerular layer. Asterisk indicates glomerulus. **b** External tufted cell in glomerular layer. **c** Middle tufted cell in external plexiform layer. **d** Interneuron in external plexiform layer. **e** Internal tufted cell nearby mitral cell layer. IPL, internal plexiform layer. **f** Mitral cell in mitral cell layer. **g** Granule cells in mitral cell layer. **h** Internal tufted cell (left) and mitral cell (right) with UEA-I-positive fiber (red lines) correspond to (**e**) and (**f**), respectively. Bars = 10 μm.

fig. 5. UEA-I binding in frontal sections of basal region of brain. Sections from male ICR mouse processed using Bouin's fixative and paraffin embedding. **a** Anterior olfactory nuclei (AON). RMS, rostral migratory stream. **b** Anterior piriform cortex (aPC) and olfactory tubercle (OT). Arrows indicate lateral olfactory tract. Left and

upper, medial and dorsal, respectively. Bars = 300 μm.

fig. 6. UEA-I binding in vomeronasal organ. Sections from male ICR mouse processed using 4% paraformaldehyde fixative and paraffin embedding. **a** Vomeronasal organ and nerves (asterisks) at low magnification. MZ indicates marginal zone between vomeronasal sensory epithelium (VNE) and non-sensory epithelium (NSE). G, vomeronasal gland; V, blood vessel. Left and upper, medial and dorsal, respectively. **b** Higher magnification of VNE. Arrows and arrowhead, UEA-I-positive cell membranes of receptor cells in middle and basal regions of VNE, respectively. *Axon bundles of receptor cells. **c** Higher magnification of MZ. Arrow, UEA-I-negative progenitor cell; dashed lines, borders of MZ. Bars = 300 (**a**) and 20 (**b** and **c**) μm.

fig. 7. UEA-I binding in sagittal section of accessory olfactory bulb. Sections from male ICR mouse processed from Bouin's fixative and paraffin embedding. **a** Glomerular reaction is uniform in 13 of 16 mice. Arrow, lateral olfactory tract; dashed line, border between rostral (r) and caudal (c) regions of glomerular layer. Left and upper, rostral and dorsal, respectively. EPL, external plexiform layer; GCL, granule cell layer; GL, glomerular layer; IPL, internal plexiform layer; VNL, vomeronasal nerve layer. **b** Region-specific reaction of glomeruli in three of 16 mice. Dashed line, border between rostral (r) and caudal (c) regions of glomerular layer. Left side is rostral, and upper side is dorsal. Bars = 200 μm.

supplemental fig. 1. Comparison of UEA-I binding under various processing conditions. Whole olfactory bulb processed under carious conditions (**a**, **d**), layer

structures of main (**b**, **e**) and accessory (**c**, **f**) olfactory bulb. Male C57BL/6J mouse, Bouin's fixative and paraffin embedding (**a**-**c**); male ICR mouse, 4% paraformaldehyde fixative and freezing section (**d**-**f**).

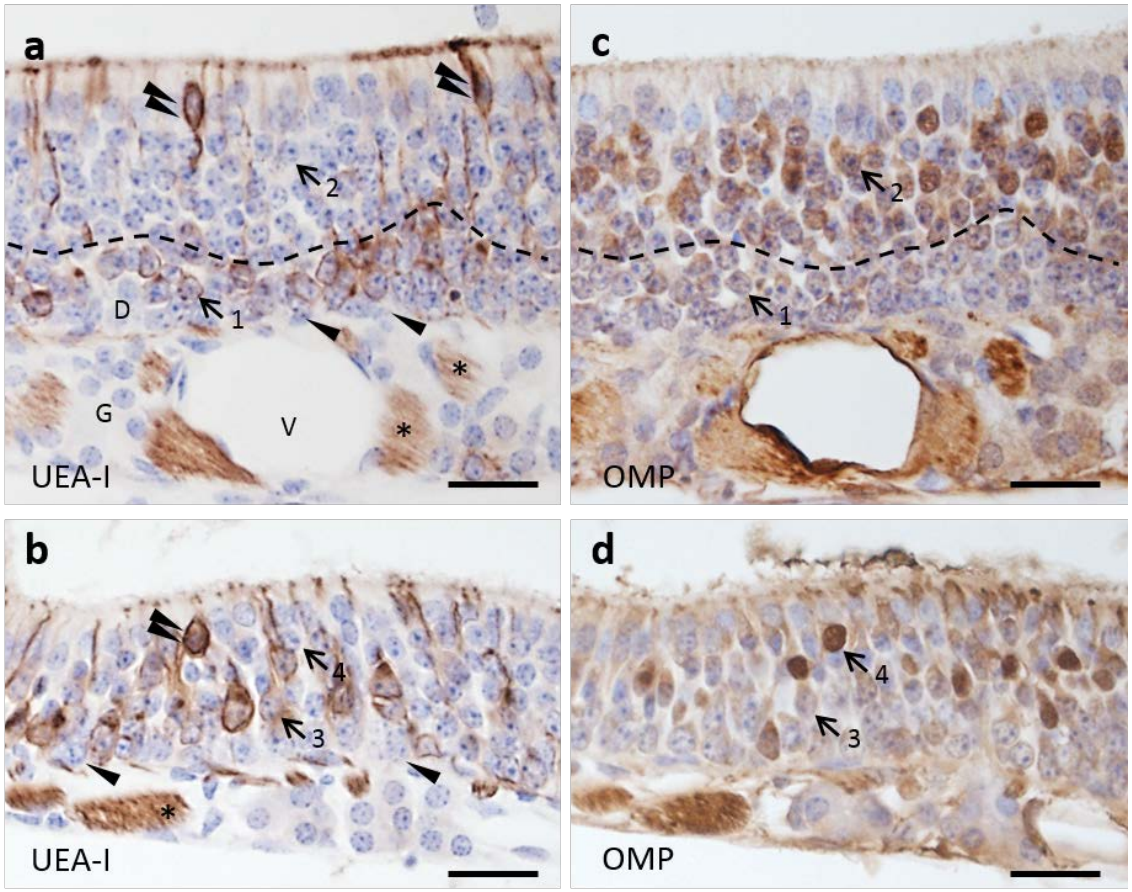

Fig. 1

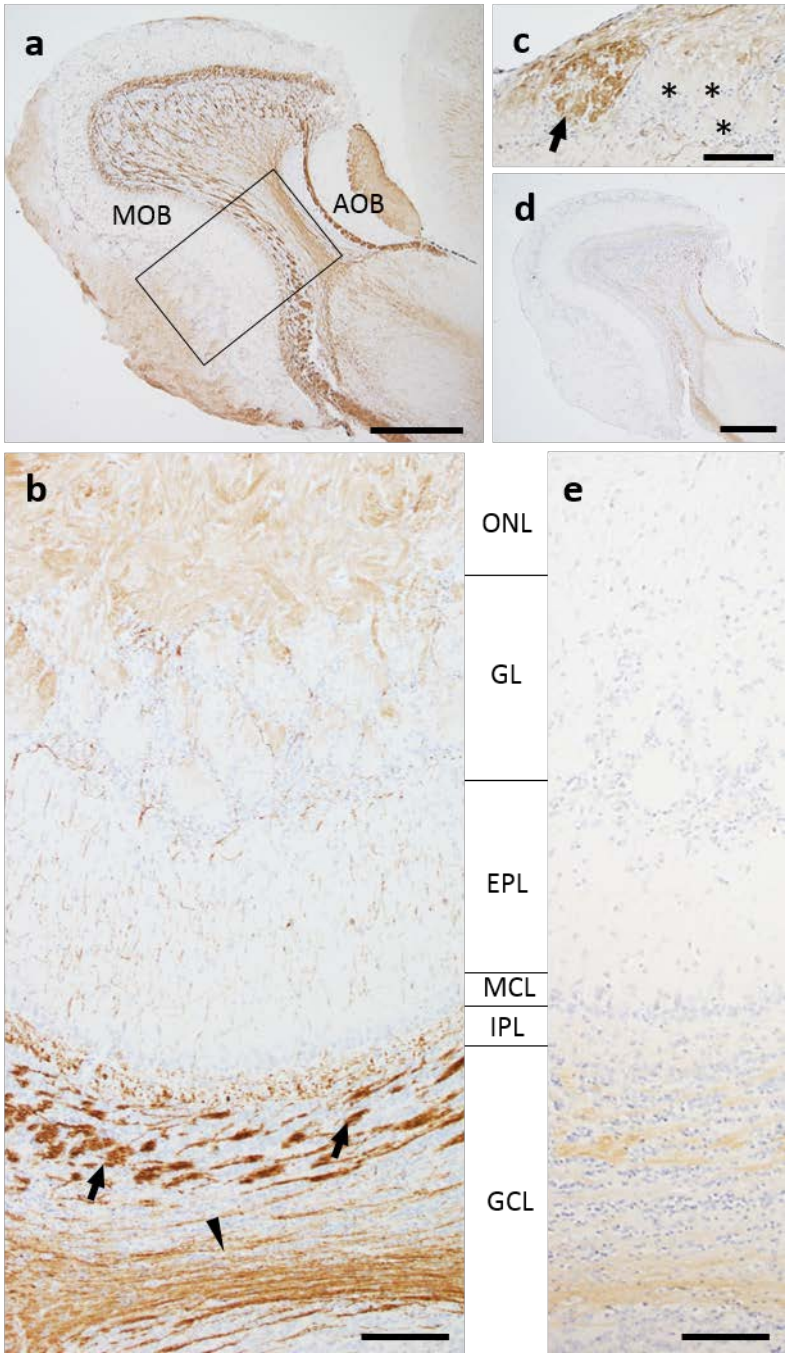

Fig. 2

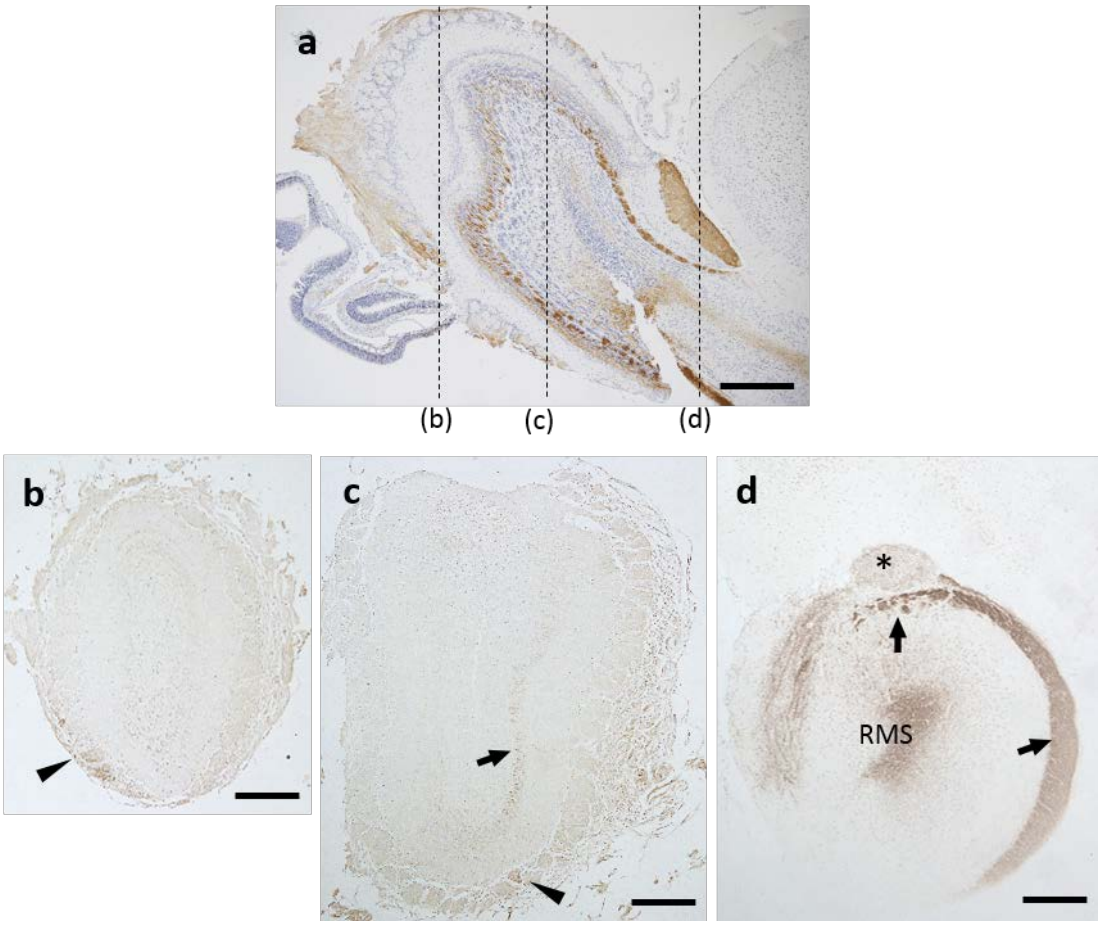

Fig. 3

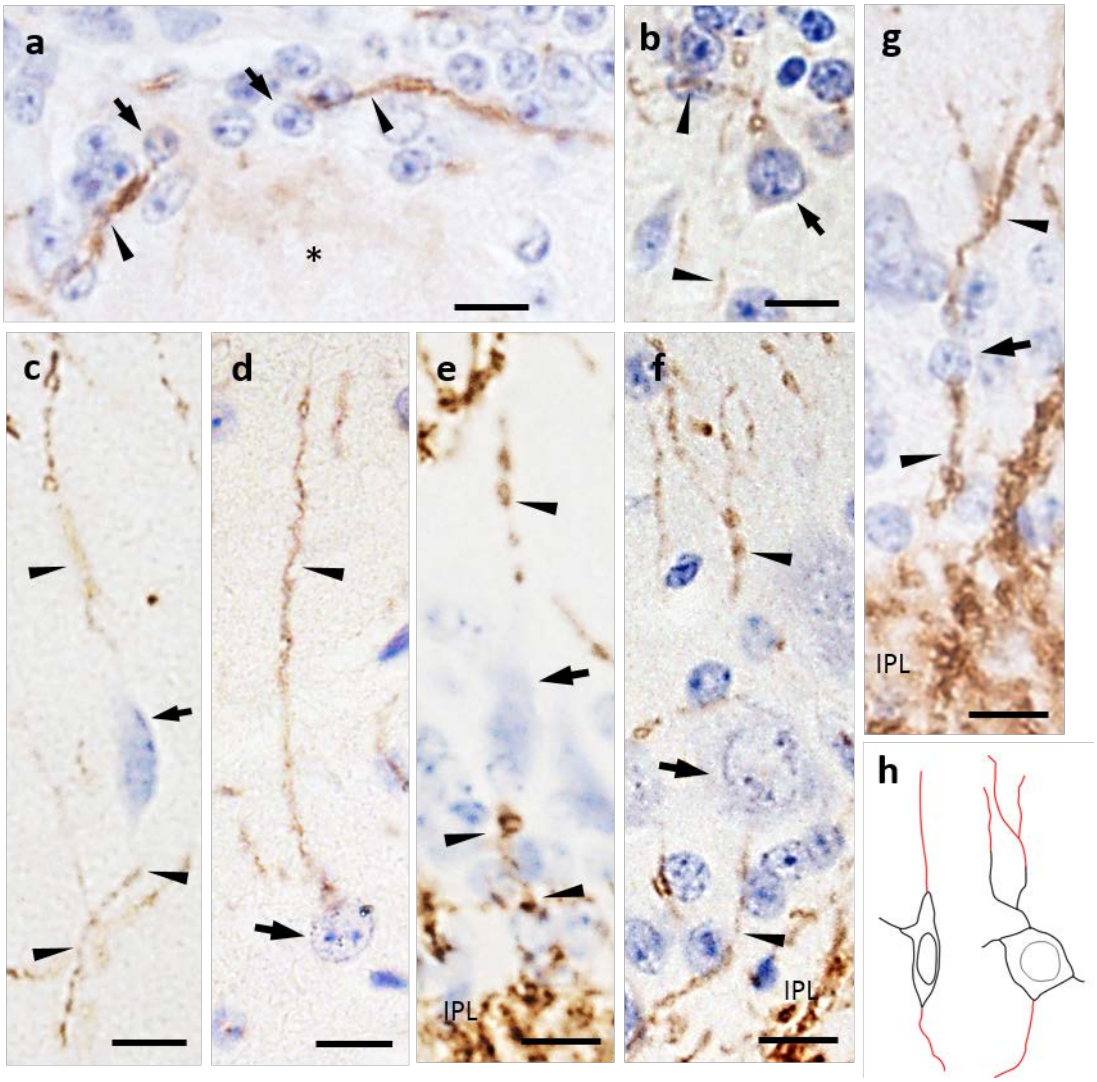

Fig. 4

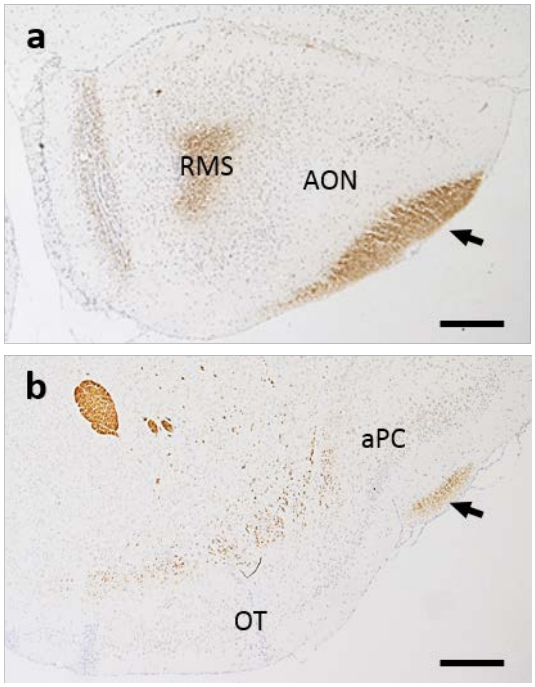

Fig. 5

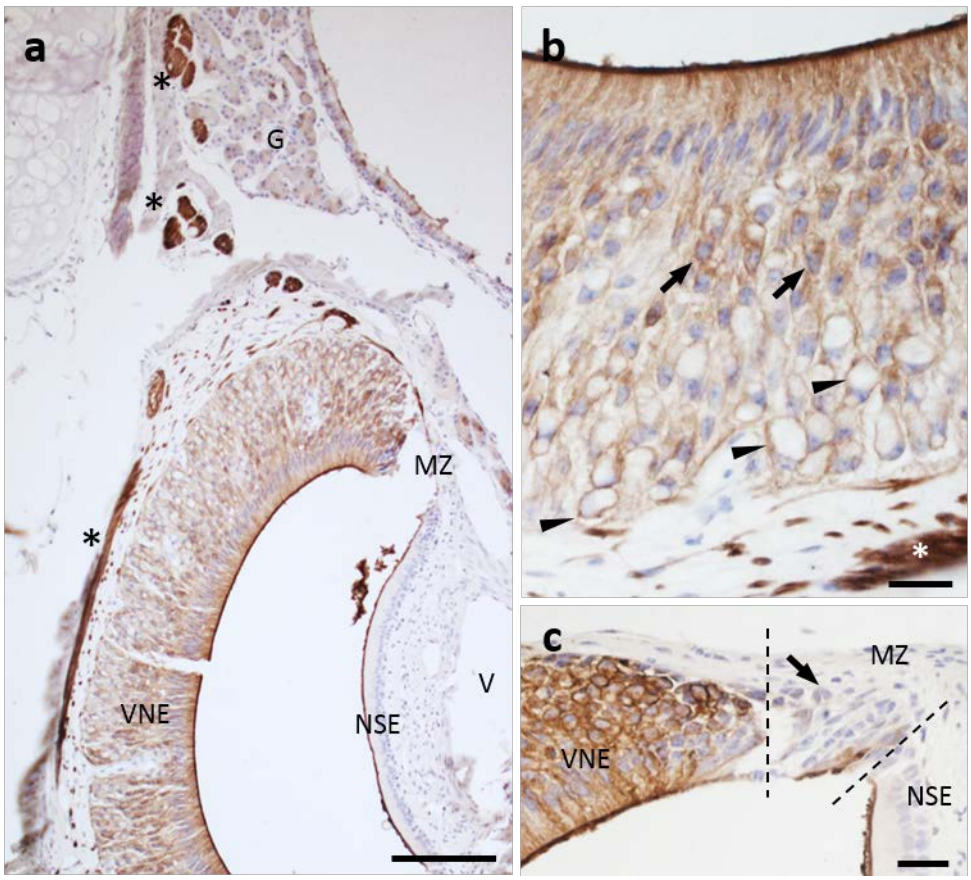

Fig. 6

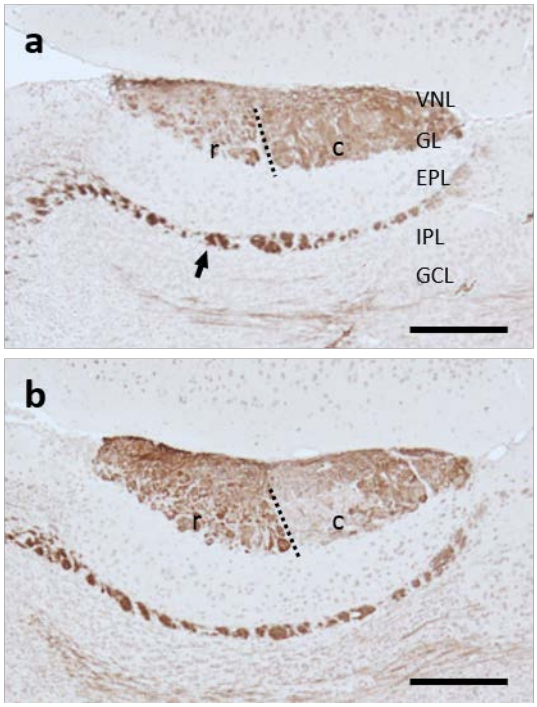

Fig. 7

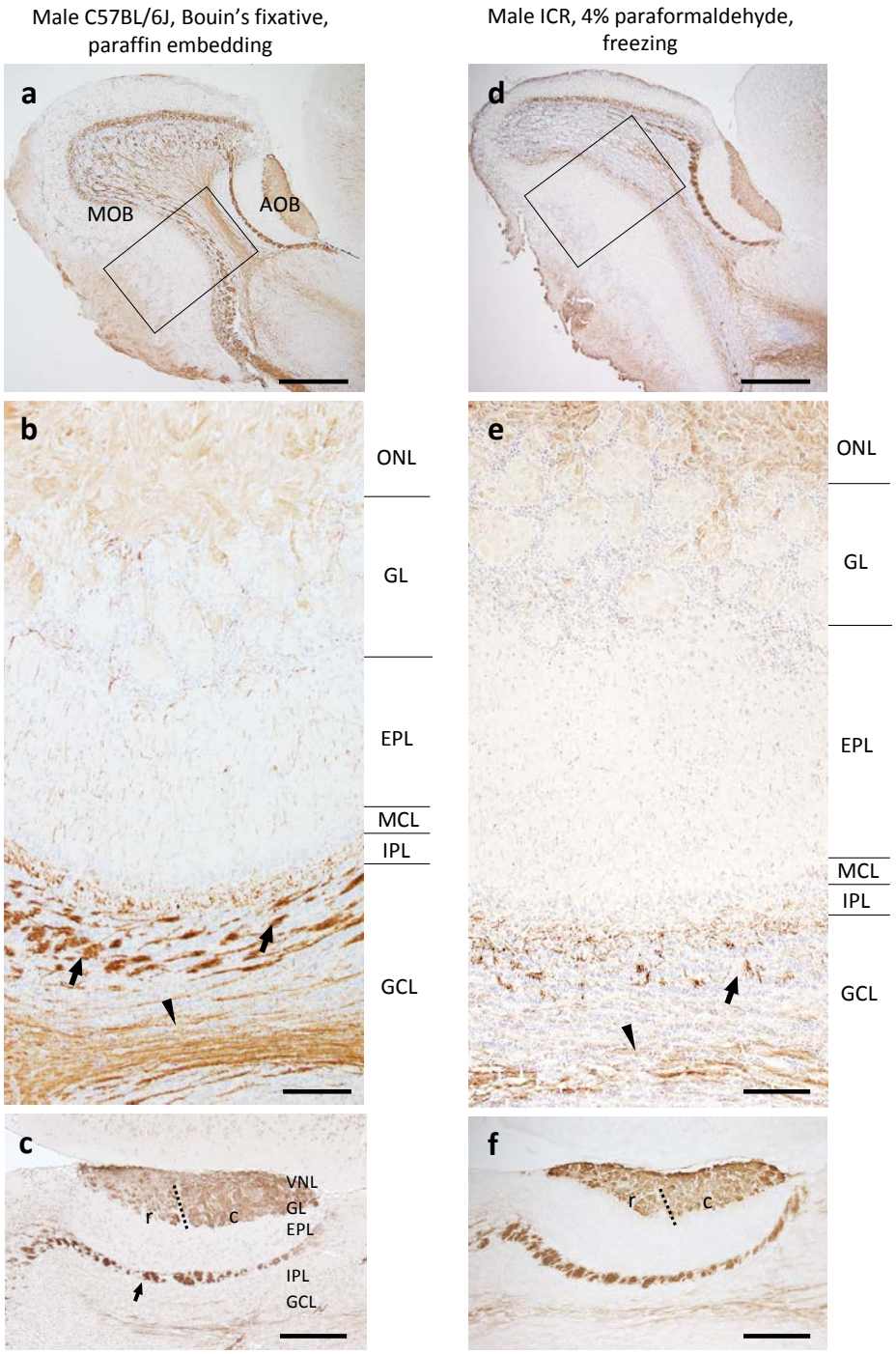

supplement fig. 1